Radar-Based Millimeter-Wave Sensing for Accurate 3-D Indoor Positioning: Potentials and Challenges

Andrey Sesyuk, *Student Member, IEEE*, Stelios Ioannou, *Member, IEEE*, and Marios Raspopoulos, *Member, IEEE*

***Abstract*—The 3-D nature of modern smart applications has imposed significant 3-D positioning accuracy requirements, especially in indoor environments. However, a major limitation of most existing indoor localization systems is their focus on estimating positions mainly in the horizontal plane, overlooking the crucial vertical dimension. This neglect presents considerable challenges in accurately determining the 3-D position of devices, such as drones and individuals across multiple floors of a building let alone the cm-level accuracy that might be required in many of these applications. To tackle this issue, millimeter-wave (mmWave) positioning systems have emerged as a promising technology offering high accuracy and robustness even in complex indoor environments. This article aims to leverage the potential of mmWave radar technology to achieve precise ranging and angling measurements presenting a comprehensive methodology for evaluating the performance of mmWave sensors in terms of measurement precision while demonstrating the 3-D positioning accuracy that can be achieved. The main challenges and the respective solutions associated with the use of mmWave sensors for indoor positioning are highlighted, providing valuable insights into their potentials and suitability for practical applications.**

***Index Terms*—3-D, indoor positioning systems, millimeter-wave (mmWave) radar.**

I. Introduction

THE explosive growth of the Internet of Things and the emergence of many location-based services (LBS) and mobile smart applications make localization an even more important key-enabling technology in the information and communications technology world while many of these LBSs impose very high 3-D localization accuracy requirements. Several approaches have been proposed during the last few decades to address the challenges of indoor localization; however, most of them only estimate positions on a horizontal ($x-y$) plane and many times neglect the vertical (z) dimension. This lack of vertical information could lead into problems, such as the inability to determine whether a device is held up high or in a pocket, etc., while accurate 3-D positioning is also critical in scenarios, such as drone-assisted crop seeding, search and rescue operations, and wireless communication [1], where submeter or cm-level accuracy is likely essential.

To address this demand, there are several technologies that are utilized for 3-D indoor positioning and all of them have their advantages and disadvantages. For instance, Wi-Fi, a technology that has been extensively utilized by either adopting fingerprinting approaches (RSS, channel state information (CSI), or fine time measurement (FTM)-based) [2], [3], [4] as well as various geometric approaches [5] is considered a technology that can be fairly easy to set up at a relatively low cost, however, it demonstrates poor accuracy in non-line-of-sight (NLOS) conditions compared to technologies like ultra-wideband (UWB). Likewise, Bluetooth, given its simplicity and inexpensiveness, is similar to Wi-Fi, however, it is prone to radio interference therefore it is typically linked with low positioning accuracy [6]. Visual light communication (VLC) and Ultrasound, despite the fact that they demonstrate relatively good accuracy compared to other technologies, they are both extremely short-ranged and applicable only in line-of-sight (LoS) situations [7], [8]. Also, audible sound, considering the fact that it is widely supported in various types of environments and able to achieve submeter level accuracy, cannot be utilized in common positioning scenarios mainly due to the disturbing noise it causes [9]. Finally, UWB and millimeter-wave (mmWave) technologies demonstrate the most promising results compared to other technologies reaching centimeter-level accuracy even in multipath scenarios and are relatively insensitive to interference. A more comprehensive survey of the technologies used for positioning can be found in [10]. Our focus on this article is on mmWave.

MmWave is currently used in some Wi-Fi systems (e.g., IEEE802.11ad) while it is planned to be used in 5G communications due to its flexibility to use wider bandwidths and hence its strong potential in achieving much higher data rates and capacity. mmWave systems typically operate in frequencies between 26 to 100 GHz. At those very high frequencies there is large availability of bandwidth which could lead to fine timing

Manuscript received 23 November 2023; revised 11 December 2023; accepted 23 January 2024. Date of publication 26 January 2024; date of current version 28 February 2024. This work was supported by the European Union through the Programme of Social Cohesion "THALIA 2021-2027", Research and Innovation Foundation under Project: CONCEPT/0722/0031. *(Corresponding author: Marios Raspopoulos.)*

The authors are with the University of Central Lancashire Cyprus, Pyla 7080, Cyprus, and also with the Center of Interdisciplinary Science Promotion & Innovative Research Exploration — INSPIRE, Nicosia 1041, Cyprus (e-mail: asesyuk@uclan.ac.uk; sioannou2@uclan.ac.uk; mraspopoulos@uclan.ac.uk).

Digital Object Identifier 10.1109/JISPIN.2024.3359151

resolution and hence high ranging accuracy. The very small wavelength also allows the development of small and compact massive phase antenna arrays that enable the accurate estimation of angles (azimuth and elevation) of arrival. All this accurate context could be used for achieving cm-level 3-D positioning accuracy or better [11]. In this work, we capitalize on the potential of mmWave technology to accurately provide ranging and angling information, and sustain the momentum of ongoing research efforts in this topic by demonstrating its suitability to achieve cm-level accuracy, while presenting the most important challenges it imposes. This work is an extended version of our work which was presented in [12].

The rest of this article is organized as follows. In Section II, the recent related works and developments in 3-D localization using mmWave technology are presented while Section III discusses the challenges and difficulties that could be faced when implementing mmWave positioning systems. Section IV describes the methodology and setup used for the experimentation using both 2-DOF and 3-DOF sensors while Section V presents the results of the 2-DOF and 3-DOF range and angle precision analysis conducted using three types of off-the-shelf mmWave sensors as well as the accuracy achieved using various approaches and critically discusses the findings. Finally, Section VI concludes this article.

II. Related Work

In response to the increasing demand for precise 3-D indoor positioning in smart applications, there has been a growing surge in research and development efforts in recent years. These efforts are aimed at exploring advanced technologies to meet this need. The authors in [10] offered a comprehensive survey of 3-D indoor localization techniques and approaches. It delves into various modern technologies, providing insights and evaluations. Notably, the authors of this article reference some works relevant to mmWave technology. While positioning research using this mmWave technology is in its early stages, early theoretical findings and practical experiments reveal its potential to deliver the high accuracy demanded by modern smart applications. Some of these works include systems which utilize a single mmWave base station setup, as described in [13], in which the authors proposed a method that fuses user equipment motion features, mmWave LoS, and first-order reflection paths' angle of arrival (AoA) and time of arrival for indoor positioning. They present an improved least mean square algorithm to refine multipath AoA estimation and a modified multipath unscented Kalman filter for position tracking. The results of these methods show significant enhancements in LoS–AoA estimation and centimeter-level 3-D positioning accuracy, around 60 cm. Notably, this strategy is effective even in scenarios with insufficient anchor nodes. A similar approach, as presented in [14], leverages multipath channels, with multiple-input–multiple-output (MIMO) antennas estimating the angles of multipath coherent signals, and orthogonal frequency division multiplexing (OFDM) signals handling delay estimation. By integrating MIMO and OFDM technologies within a wireless communication system, an array antenna is employed to estimate the AoA of multipath signals. Spatial smoothing algorithms are applied in the frequency domain to estimate the time difference of arrival (TDoA) of multiple coherent signals. This approach has been validated through simulations in a $6 \times 8 \times 4.5$-m indoor space. The results indicate that positioning accuracy using a single sensor reaches submeter levels in 95% of cases and is less than 0.4 m in 60% of cases. The richness of multipath components in mmWave systems is also exploited in [15] which introduces a multipath-assisted localization (MAL) model based on mmWave radar for indoor electronic device localization. This model effectively incorporates multipath effects when describing reflected signals, enabling precise target position determination using the MAL area formed by the reflected signal. Importantly, this model can provide 3-D target information even when traditional single-input–single-output radar falls short. A 60-GHz signal-based positioning and tracking system is discussed in [16], which effectively filters out multiple reflections and diffuse scattering, ensuring a high level of accuracy. Operating within a longitudinal range of 0.46–5.55 m and a lateral span from 1.91–3.04 m, the system determines the target's position through the calculation of the local centroid in the associated point cloud. Overall, the system achieves a plane positioning accuracy with a 99% confidence level and an error of approximately 30–40 cm. Another work utilizing an AoA approach is proposed in [17] in which the authors conduct AoA and signal measurements in a 35×65.5-m open space, achieving position accuracy ranging from 16–3.25 m. A hybrid approach is presented in [18], where a novel 3-D indoor positioning scheme using mmWave massive MIMO (mMIMO) systems is based on the combination of received signal strength and AoA (RSS-AoA) positioning scheme, which employs only a single access point equipped with a large-scale uniform cylindrical array. The authors designed a novel hybrid RSS-AoA positioning scheme for the computations of the 3-D coordinates of the target mobile terminal. They demonstrated that their approach achieves azimuth and elevation precision around 0.5° depending on the quality of the received signal.

Reconfigurable intelligent surfaces (RIS), renowned for their ability to controllably manipulate radio propagation are also gaining attention from researchers working on positioning. For instance, in [19], the authors investigate a 3-D positioning algorithm for a mmWave system leveraging RIS, to enhance the positioning performance of mobile users (MUs). They use a two-stage weight least square (TSWLS) algorithm to obtain the closed-form solution of the MU's position. Similarly in [20], the authors address the channel estimation for RIS-aided mmWave communication systems based on a localization method. They propose the concept of reflecting unit set (RUS) to improve the flexibility of RIS. The authors then propose a novel coplanar maximum likelihood-based 3-D positioning method based on the RUS and derive the Cramér–Rao lower bound (CRLB) for the positioning method. Furthermore, they develop an efficient positioning-based channel estimation scheme with low computational complexity. They demonstrate that cm-level accuracy can be achieved averaging around 5 cm depending on the received signal quality.

Drone 3-D localization is popular within the research community. For example, in [21], the authors presented a self-localization system for autonomous drones that utilizes a single mmWave anchor. The system leverages a novel dual polarized, dual modulated mmWave anchor and mmWave-IMU fusion

self-localization algorithm to achieve precise, high-speed 3-D localization. The authors have demonstrated a median localization error of 7 cm and a 90th percentile less than 15 cm, even in NLOS scenarios. The authors in [22] presented an active drone detection system that uses a mmWave radar mounted on a drone to estimate 3-D position of a drone using 2-D measurements. The results indicated an average 3-D positioning error of 2.17 m. In [23], the authors developed a 3GPP-compliant drone-based 3-D indoor localization solution employing an integration of time-based and angle-based techniques to improve the situational awareness in emergency situations and support emergency services. They have managed to achieve a horizontal and vertical positional error 1.05 and 0.7 m at 26 GHz. A similar work is presented in [24] where the authors proposed a security system based on an mmWave radar, using a processing workflow based on machine learning techniques, achieving 99.32% accuracy and 99.54% F1 score. Another work utilizing machine learning is presented in [25], where a custom convolutional neural network (CNN) model achieves an accuracy of 95%.

Other interesting works include [26], where the authors theoretically derived the Cramér–Rao Bound for position and rotation angle estimation uncertainty using mmWave signals from a single transmitter, even in the presence of scatterers. They demonstrate that under open LoS conditions, it is feasible to estimate a target's position and orientation angle by leveraging information from multipath signals. However, this approach comes with a noticeable performance penalty. In addition, the authors in [27], showcased the advantages of array antennas in determining a device's orientation. Notably, the accuracy of mmWave technology-based positioning appears to be closely linked to the distance from the target.

III. Challenges

During the development and setup of the positioning system described in this work, several challenges have emerged regarding the usage of mmWave sensors which could potentially cause significant difficulties when these are used for positioning. This section describes all these challenges and subsequently explains the solutions we implemented to overcome them.

1) Accuracy and Sensing: Although mmWave sensors have been introduced to be used mainly for ranging measurements for the automotive industry, they have emerged as a promising radar-like technology for indoor positioning applications due to their high accuracy in estimating distance (and angles) to objects mainly because of the availability of a very wide bandwidth on mmWave frequencies and the availability of phase antenna arrays on the sensor board. However, the accuracy of mmWave sensors is highly dependent on the sensing conditions, such as the scattering caused due to reflective surfaces, the angle of incidence, and the distance between the sensor and the target object. In addition, the complexity of the indoor environment including multipath effects, can affect the accuracy of mmWave sensing. Therefore, careful consideration of the sensing conditions and the deployment of mmWave sensors is essential to achieve high accuracy in indoor positioning applications. Our experimentation has indicated that the presence of metallic objects in the close vicinity of the target or within the field of view of the sensor causes problems.

2) Stationary Positioning: In addition to the sensing constraints, the fact that these sensors rely strongly on the Doppler-effect principle, challenges emerge when stationary targets need to be detected. To be sensed by a mmWave radar sensor, an object must be constantly in motion for the sensor to be able to detect the Doppler shift and distinguish it from stationary objects and background noise. To overcome this challenge, researchers are currently exploring several approaches. One promising solution could be the fusion of mmWave data with information collected from inertial sensors. For our experiments, this limitation was overcome since the continuous rotation of the propellers of the drone turned out to be beneficial as it causes micro-Doppler effects [28].

3) Multiobject Detection/Clustering: An inherent limitation of the off-the-shelf mmWave sensors compared to systems that use receivers on the target is the fact that they operate based on the radar principle reducing the capability of identifying correctly specific objects. The mmWave sensor emits electromagnetic waves at high frequencies that bounce off surrounding objects and return as echoes. By analyzing the time delay and amplitude of these echoes, the sensor can determine the location and characteristics of the objects in the environment relative to each sensor. These echoes, however, can become mixed together in complicated environments with multiple objects, making it difficult to differentiate and identify specific objects. This becomes especially more challenging when using multiple sensors to identify a position of a specific object in the presence of other moving or stationary objects. The solution to this multiobject identification is clustering. Literature reports various clustering approaches that can be used for this purpose [29], [30], [31].

The clustering technique used in this work to identify a specific target is known as the z-score method [32], which is widely employed for identifying and managing outliers in datasets. This method begins by calculating the mean and standard deviation of the dataset and then computes the z-score for each data point, measuring its deviation from the mean in terms of standard deviations. By establishing a threshold, typically based on a certain number of standard deviations away from the mean, outliers can be identified and subsequently removed from the initial detected objects list to obtain a new filtered list of clustered points.

The ability of the mmWave sensors (like the Texas Instruments IWR1642BOOST) to measure the relative range and azimuth of a detected object facilitates this clustering process as it allows the estimation of the relative (x, y) coordinate of the target. As this target is detected from multiple sensors its relative coordinates need to be converted to absolute ones by utilizing the rotation/translation equations shown below [(1) and (2)] in which θ is the absolute orientation of the sensor and $x_{\text{trans}}, y_{\text{trans}}$ are the 2-D coordinates of each sensor relative to the chosen 0,0 point. Once this is done, the measurements from each sensor correspond to the same axes system, and their (x, y) coordinates can be matched to identify the range/angle measurements from

the multiple sensors to the same object

$$x_{\text{abs}} = x\cos\theta + y\sin\theta + x_{\text{trans}} \quad (1)$$

$$y_{\text{abs}} = -x\sin\theta + y\cos\theta + y_{\text{trans}}. \quad (2)$$

The analogous clustering process for IWR1843BOOST sensors closely mirrors the aforementioned methodology considering also the z-dimension in the clustering process as these sensors additionally measure the elevation angle to the target. Similar to the IWR1642BOOST, these relative coordinates are translated to a common axis system by utilizing the equations mentioned in Section V-B2a, ensuring uniformity across sensor data. Subsequently, the z-score method is employed here too to eliminate outliers.

4) Timing Synchronization: Timing synchronization is critical in mmWave positioning systems that use multiple sensors to accurately determine the location of objects. When multiple sensors are used, they must be synchronized so that they can collectively capture and analyze the echoes returned from the environment. If the sensors are not synchronized, the echoes may arrive at different times, leading to incorrect and inconsistent measurements, which can result in inaccurate positioning data. The timing synchronization ensures that the sensors are accurately aligned in time, allowing them to capture the echoes simultaneously and consistently. Therefore, timing synchronization is critical to the performance and accuracy of mmWave positioning systems.

To achieve timing synchronization, a timestamp was placed at the beginning of each data string. The timestamp corresponds to the exact recording time, allowing for accurate alignment with the real-time clock. By matching these timestamps with the current time, the data strings within a specific timeframe were then organized into a list. Once the data string list is established, it is then filtered using the clustering technique mentioned previously and utilized to identify a specific object within the environment. At the beginning of each positioning session all the hosts in the setup update their time using the same universal clock over the Internet.

5) Placement and Orientation of the Sensors: When it comes to maximizing the effectiveness of mmWave radar devices in capturing the best field of view for a given scene of interest, several key best practices come into play. These practices are particularly crucial when dealing with varying room dimensions and aiming to calculate the most optimal sensor orientation to cover the majority of a room. First, it is essential to consider the room dimensions. The size and shape of the space significantly impact the placement and angle of mmWave sensors. In larger rooms, positioning sensors in multiple corners or along the walls can help achieve better coverage. In contrast, smaller rooms may require a more centralized placement to prevent blind spots. In addition, understanding the reflective properties of the room's surfaces, such as walls, floors, and objects within the room, can aid in optimizing sensor placement. These reflective surfaces can impact the propagation of radar waves and affect the device's ability to detect objects accurately. When aiming to capture the majority of the room from a corner, to maximize coverage, angling the radar device in a way that covers a wide field of view is crucial. This can often be achieved by tilting the sensor downward slightly from the corner and orienting it to cover both the horizontal and vertical dimensions of the room. Adjusting the sensor's vertical tilt allows it to detect objects closer to the floor and higher up, ensuring comprehensive coverage within the room.

Moreover, in scenarios where precision is paramount, employing multiple mmWave radar devices with varying angles and orientations can be beneficial. These devices can complement each other's coverage and reduce the likelihood of missing objects or obstructions. When setting up an mmWave multilateration positioning system, it is essential to pay attention to the dilution of precision (DOP) and specifically the vertical DOP (VDOP) when trying to achieve 3-D positioning accuracy. DOP plays a crucial role in 3-D indoor positioning, as it directly affects the accuracy and reliability of position estimates [33]. While DOP values are commonly considered in the horizontal plane, they are equally important in the vertical plane [34]. A key approach to optimizing DOP involves strategically selecting and configuring the positioning of the sensors in the system. By optimizing the spatial distribution of these sensors, the geometric configuration is enhanced, leading to lower DOP values. This, in turn, results in improved accuracy and reliability of the position solution. Furthermore, the integration of additional sensors can be strategically employed to enhance the accuracy and robustness of the 3-D positioning system.

IV. Methodology

A. System Overview

The methodological framework to investigate the research question posed in the introduction is presented in this section, describing the experimental system setup and equipment used while considering the particular challenges that the available mmWave products impose toward achieving the desired 3-D accuracy. The current market availability of mmWave radar sensors has steered this investigation in mainly two directions: one using two degrees-of-freedom (2-DoF) sensors that support ranging and azimuth measurements and one using 3-DoF sensors that additionally measure the elevation of targets. For each of these cases we performed a precision analysis of the most predominantly used mmWave ranging sensors currently in the market, and thereafter used the ranging/angular information to conduct positioning using various methods.

B. 2-DOF Sensor Setup

1) Equipment: The two mmWwave radar sensors that were used for the 2-DOF precision analysis were the Texas Instruments (TI) IWR1642BOOST and Infineon Distance2Go. The TI sensor is equipped with four receiving (Rx) and two transmitting (Tx) antennas operating at frequencies between 76–81 GHz with a 120° field of view and ranging capabilities of up to 72 m. In contrast, the Infineon Distance2Go mmWave sensor is equipped with one Rx and one Tx antenna and operates between 24–26 GHz with a field of view of 20° and a maximum detection range of around 20 m. While the TI sensor performs range and

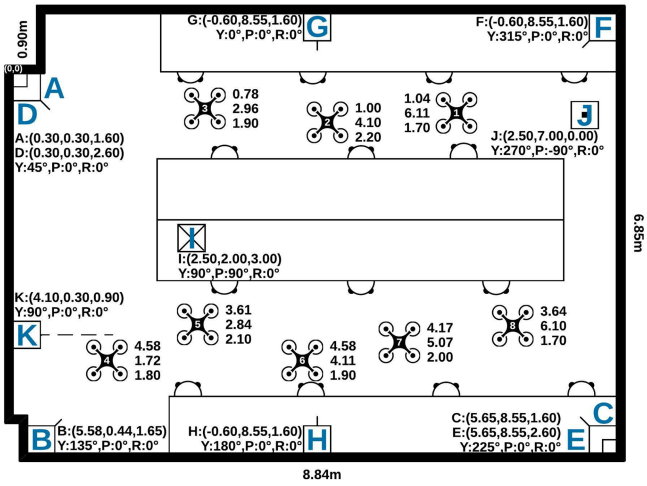

Fig. 1. mmWave 3-D positioning experimental setup using 2-DOF mmWave sensors (Y: Yaw, P: Pitch, R: Roll).

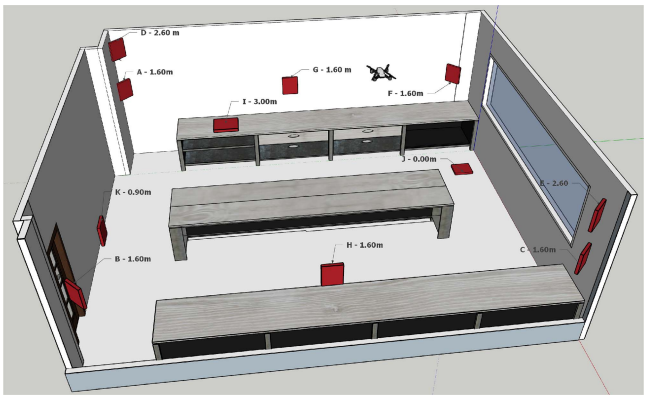

Fig. 2. mmWave 3-D positioning experimental setup using 2-DOF mmWave sensors (3-D view).

angle measurements, the Infineon one can only measure range. The experimental setup involved utilizing a DJI Air 2S drone as the target for ranging and angular measurements. It is a compact drone with dimensions of 183.0 ×77.0 × 253.0 mm.

2) Experimental Setup: Both the precision analysis and the 3-D positioning accuracy experimentation using 2-DOF sensors were carried out in an 8.85×6.85-m engineering laboratory, the top-view of which is shown in Figs. 1 and 2. The precision analysis was conducted to compare the ranging and angular capabilities of the two mmWave sensors. In this analysis, the sensor under test was placed in location **K** and range measurements were collected every 0.5 m while the drone was flying in a straight line in front of the sensor (0.5–8 m). To assess the ability of the sensors to conduct range measurements at different angles, the orientation of the sensor was systematically varied from 0–60° (15° step). This comprehensive analysis aimed to gather precise data on the sensors' precision, resolution, and reliability at different distances and angles. Also, the precision of the TI sensor in measuring the angle of departure was evaluated using the same setup.

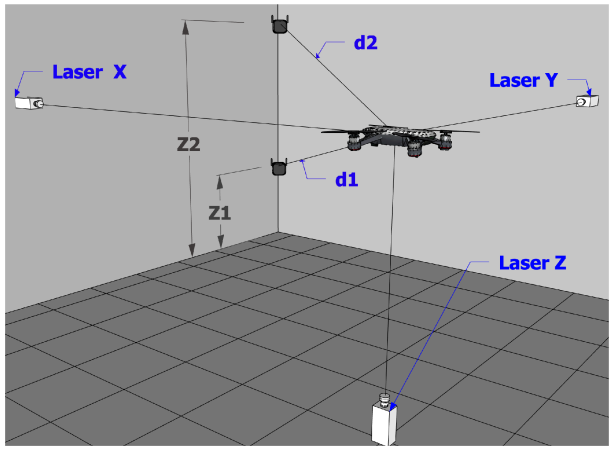

Fig. 3. Laser-based positioning of the drone on ground truth locations.

For positioning accuracy experimentation, the positioning system comprises mainly of a number of TI mmWave sensors each of which is connected to a Raspberry Pi 4 that serves as a gateway collecting the data from each TI sensor and sending it to the central PC for processing. Each sensor has its own Raspberry Pi 4 where the data string is sent through a UDP connection and parsed. A number of TI sensors were deployed in various locations within the lab (indicated with different capital letters in Fig. 1 while position estimation was done using three approaches: 1) 3-D algebraic multilateration, 2) 3-D recursive multilateration, and 3) an improved 3-D-triangulation approach. Different combinations of sensors were used for each case to investigate the effects of DOP. Eight ground-truth points (**1–8**) were randomly selected across the lab space. Each point was meticulously marked, and their corresponding coordinates were recorded. The drone was positioned precisely on these marked points and subsequently lifted to hover over them at various heights. To ensure the precision of positioning the drone at the exact ground truth location, three laser pointers were positioned along the x, y, and z axes of that location pointing toward the drone, as shown in Fig. 3. The drone was let to hover still once the laser focus point from the three lasers appeared in the center of the drone which is considered the drone real location. While the drone was at each measurement location, the range and angle measurements from each sensor were sent to a central PC that produces the metadata needed to perform 3-D positioning calculations using the two approaches mentioned above. For all the measurements conducted in this article a set of 10 mmWave readings were collected from each sensor at every drone location, which were then averaged excluding possible outliers using the z-score approach. This setup allowed for a direct comparison of the accuracy and performance of the two methods for real-time 3-D positioning, providing valuable insights into capabilities and suitability for both the methods and the technology for practical applications.

C. 3-DOF Sensor Setup

1) Equipment: Similarly to IWR1642BOOST, the IWR18-43BOOST possesses a frequency modulated continuous wave

Fig. 4. mmWave 3-DOF precision analysis setup using 3-DOF mmWave sensors.

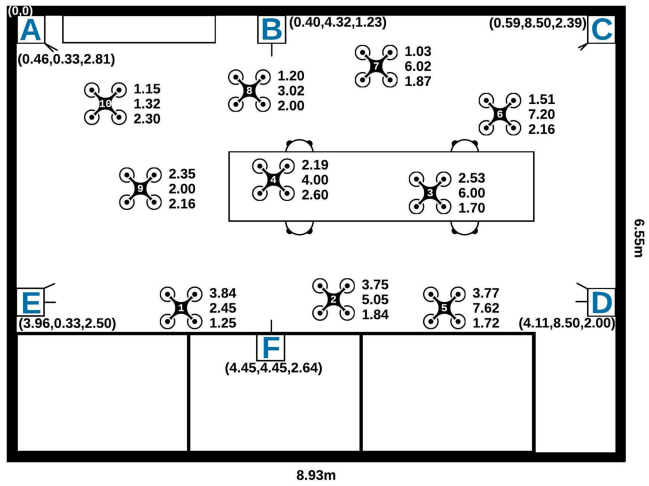

Fig. 5. mmWave 3D positioning experimental setup using 3-DOF mmWave sensors.

transceiver which enables the measurement of range, azimuth angle, and velocity of the target. However, due to an additional TX antenna, in addition to the azimuth angling information, it is also able to provide the elevation data of the target. A similar system setup was used for this setup like the one used for the IWR1642BOOST in which each sensor is connected to a Raspberry PI that parses the collected context and sends it to a central PC through a UDP connection.

2) Experimental Setup: An experiment utilizing IWR1843BOOST mmWave sensors was performed to conduct a 3-DOF precision analysis to assess the sensor's performance under various azimuth and elevation angles. As it can be seen in Fig. 4 the mmWave sensor, mounted on a versatile tripod that allowed both vertical and horizontal adjustments, provided an ideal platform for manipulating the sensor's orientation. In contrast to the setup in Section IV-B2, where the drone was systematically moved away from the sensor, in this setup, the drone was stationary positioned at a specific point while the tripod used moved at different distances away from the target (0–6.5 m). The azimuth angle, representing the horizontal orientation, and the elevation angle, representing the vertical orientation, were adjusted to different degrees to test the sensor's precision under diverse angling conditions. This comprehensive approach aimed to uncover any potential limitations or strengths of the mmWave sensor in different spatial configurations.

In the pursuit of advancing positioning experiments, a 3-DOF positioning accuracy experiment was conducted utilizing the IWR1843BOOST, similar to 2-DOF experiment that employed the IWR1642BOOST mmWave sensors where the drone was hovered across multiple scattered points across the room. This exploration took place in a separate laboratory setting (see Figs. 5 and 6), emphasizing the versatility and adaptability of the sensor systems across different environments. To ensure a comprehensive assessment of the system's capabilities, the sensors were mounted on adaptable tripods, allowing for flexibility in placement and orientation. Two distinctive sensor setups,

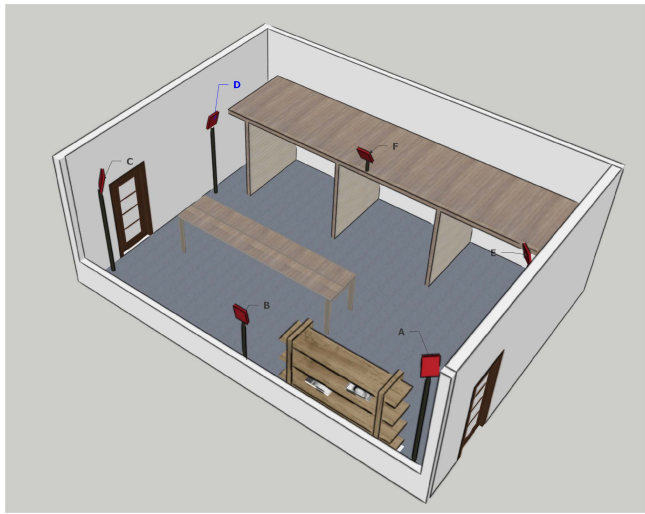

Fig. 6. mmWave 3-D positioning experimental setup using 3-DOF mmWave sensors - 3-D view.

denoted as Setup A and Setup B, were meticulously devised to examine varying anchor configurations and orientations. In Setup A, two sensors were strategically positioned in the corners, facing diagonally toward the center of the room, while two additional sensors faced each other in parallel to the wall. This configuration aimed to optimize room coverage, with a slight downward tilt applied to enhance the spatial perception of the environment. In addition, a fifth sensor was centrally placed along one of the walls, oriented upward to capture data from an alternative perspective. Setup B featured four sensors situated in the corners and oriented diagonally toward the central point of the room. This arrangement was specifically designed to enhance coverage of the central area, with a deliberate tilt to maximize the effectiveness of the system. In this setup, a fifth sensor was strategically elevated and directed downward, compared to the upward orientation in the previous arrangement. The details of these two setups are tabulated in Table V.

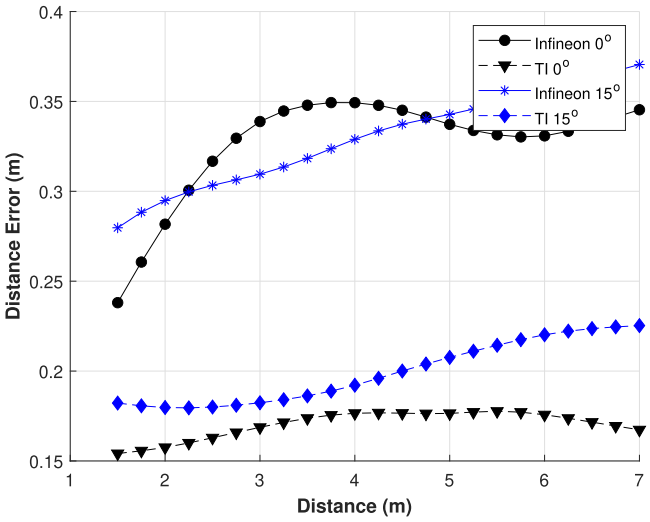

Fig. 7. Infineon versus TI distance accuracy.

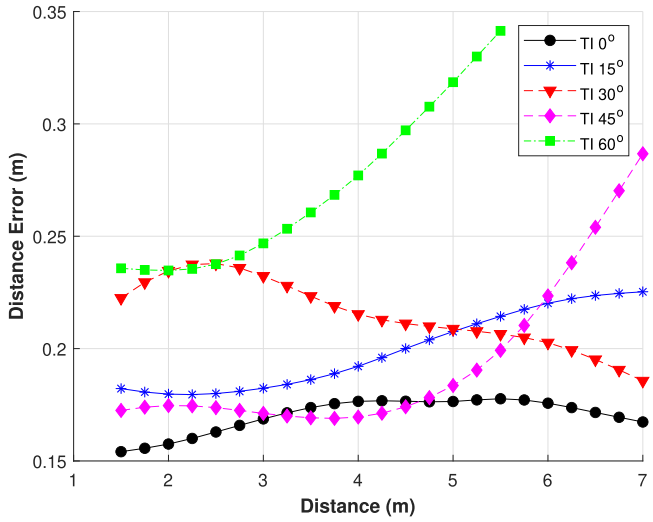

Fig. 8. IWR1642BOOST distance accuracy.

V. Results

A. 2-DOF Sensor

1) Precision Analysis: To evaluate the accuracy and sensing quality of the IWR1642BOOST and the Infineon sensors a range/angle precision analysis experimentation was carried out using the setup described in Section IV-B2. A drone was flown along a straight line, while a mmWave sensor was placed at different orientations at location **K**, as shown in Fig. 1. Given that the Infineon sensor has a relatively narrow field of view (around 20°), the analysis of distance accuracy in comparison to the TI sensor was conducted up to 15°.The results of this comparison are shown in Fig. 7 and a notable observation is the difference in distance errors between the two sensors. Both at 0° and 15°, the TI sensor outperforms the Infineon sensor. Specifically, the TI sensor demonstrates an average distance error of around 0.17 m, whereas the Infineon sensor exhibits a higher error of 0.32 m. While the error remains relatively consistent as the distance increases for both sensors, the analysis indicates a decrease in accuracy with larger angles. At 15°, there is a slight increase in error, approximately 0.05 m, compared to the error at 0°.

Following the comparison between the two sensors, the distance and azimuth angle accuracy of the TI sensor were further tested beyond 15°, as depicted in Figs. 8 and 9. Fig. 8 specifically illustrates the distance error of the TI mmWave sensor across angles ranging from 0–60°.

Upon closer inspection, it becomes evident that while the error remains consistent for each analyzed angle, there is a noticeable and constant increase in error. At 0°, the average distance error stands at 0.17 m, gradually rising to approximately 0.32 m at 60°. It is worth noting that considering the wide field of view spanning 60°, an error of 0.17 m may not appear excessively large. However, a limitation is encountered as the sensor ceases to detect objects beyond a range of 6 m.

Following the range-precision analysis, an experiment was conducted to evaluate the azimuth angle precision of the TI sensor. Similar experimental methodology was used, with the object moving away from the sensor while adjusting the sensor angle from 0°–60°. The results can be seen in Fig. 9. During the experiment, the azimuth angle error exhibited variations ranging from 0.5°–3.5°. Notably, it was observed that the error improved with increasing distance. This improvement can be attributed to the fact that as the object moves farther away, its target size diminishes, making it relatively easier to identify accurately.

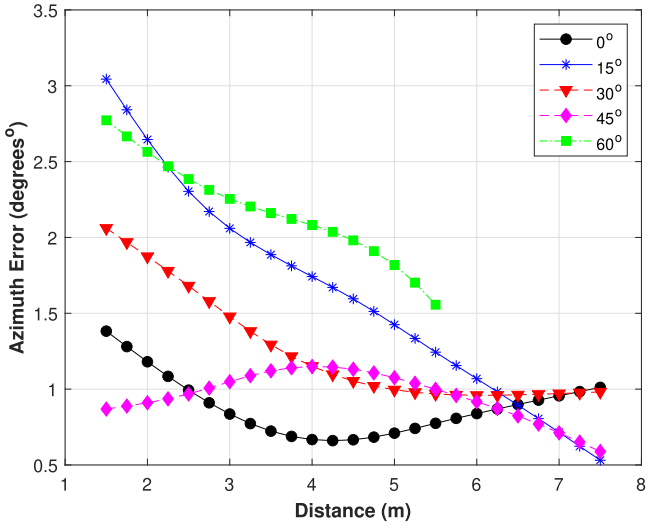

Fig. 9. IWR1642BOOST azimuth accuracy.

2) 2-DOF Sensor 3-D Positioning: Utilizing the experimental setup described in Section IV-B2, a set of ranging and angular measurements was collected from TI mmWave sensors while the drone was flown at eight well-known 3-D locations, as shown in Fig. 1. Using these measurements 3-D positioning estimation was conducted both using a two 3-D multilateration and a triangulation approach. The Ground-truth location precision is crucial for the validity of this work as it serves as the reference for evaluating the accuracy of the approach. While flying around the lab, the drone was instructed to hover at the particular points of

interest and while hovering the precise location of the drone was determined using laser pointers placed on both perpendicular walls and the floor (as seen in Fig. 3), the cross-section of which determined the exact point at where the drone must be hovered. When taking into account the position of the drone, specifically the center of the drone was considered as the real position to be derived. The utilization of a drone as the positioning target presents a significant advantage for the mmWave sensor in its identification capabilities. The dynamic nature of the drone, particularly the rotation of its propellers, induces a micro-Doppler shift in the signals received by the sensor [28]. This micro-Doppler shift phenomenon arises from the motion of scattering objects, in this case, the rotating propellers, causing a change in the frequency of the reflected signals as previously mentioned in Section III.

a) 3-D multilateration approach: Multilateration serves as a fundamental technique for achieving 3-D positioning across a wide range of scientific and technological domains. It harnesses distance measurements from multiple reference points to determine the exact location of an object within 3-D space by using at least four sensors. Through the exploitation of geometric relationships between the object and these reference points, multilateration algorithms facilitate the calculation of intersecting spheres or hyperboloids, ultimately yielding the object's coordinates. In this work, 3-D position estimation is done using the standard algebraic solution [35] of the 3-D multilateration problem, where the unknown 3-D position $\mathbf{p}_i = (x_i, y_i, z_i)^T$ is calculated algebraically given their relative distance measurements $d_{i,j}$ to a set of k anchors with known coordinates denoted as $\mathbf{P}_n j = (x_j, y_j, z_j)^T$. The formulation of this approach is as follows:

$$\mathbf{A}_{(k-1)\times 3}\mathbf{p}_i = \mathbf{D}_{(k-1)\times 1} \tag{3}$$

where

$$\mathbf{A} = \begin{pmatrix} (x_k - x_1) & (y_k - y_1) & (z_k - z_1) \\ (x_k - x_2) & (y_k - y_2) & (z_k - z_2) \\ \vdots & & \\ (x_k - x_{k-1}) & (y_k - y_{k-1}) & (z_k - z_{k-1}) \end{pmatrix}$$

$$\mathbf{D} = \frac{1}{2}\begin{pmatrix} d_{i,1}^2 - d_{i,k}^2 + x_k^2 - x_1^2 + y_k^2 - y_1^2 + z_k^2 - z_1^2 \\ d_{i,2}^2 - d_{i,k}^2 + x_k^2 - x_2^2 + y_k^2 - y_2^2 + z_k^2 - z_2^2 \\ \vdots \\ d_{i,k-1}^2 - d_{i,k}^2 + x_k^2 - x_{k-1}^2 + y_k^2 - y_{k-1}^2 + z_k^2 - z_{k-1}^2 \end{pmatrix}.$$

The algebraic solution is compared to the recursive multilateration approach presented in [36]. Unlike the traditional algebraic multilateration method described above, which estimates the position of an object based on distance measurements from multiple reference points, recursive multilateration refines its position estimation iteratively by using a recursive least square approach which attempts to find the most optimal solution. The recursive approach starts by estimating a the position using three known anchors while measurements from additional anchors are gradually introduced (if available) until all anchors have been added. Every iteration includes the estimation of a new position and from this new position estimate, the distance to all the known anchors is calculated and compared to the actual distance measurements. The sum of the squared distance errors forms the metric that needs to be minimized to return the optimal solution. However, we have noticed that in several random cases, this approach fails to return an optimal solution, leading to high 3-D positioning errors, as shown later.

Different combinations of sensors were used to investigate the effects of DOP. The first experiment was conducted using ranging measurements collected from four TI sensors deployed in the four corners of the room in locations **A, B, C,** and **F**, as shown in Fig. 1 and the results for both the standard algebraic solution as well as the recursive one are tabulated in Table I. It appears that an average error in the ranging measurement of 0.06 m translates into a 0.14- and 0.1-m average positioning error in x and y using the standard algebraic solution while a considerable error is observed in the z-axis (5.72-m average). These are translated into an average 3-D positioning error of 5.76 m. The results appear to improve when using the recursive multilateration approach (vertical error of 1.69 m and an average 3-D error of 1.72 m), however, the error in the vertical dimension still remains significant. This is attributed to the fact that all sensors are placed on the same height resulting in a very high VDOP averaging around 23.6.

The reason why our results often exhibit better accuracy in the horizontal plane compared to the vertical plane can be attributed to the distribution of sensors. In the horizontal plane, the sensors are spread out more widely, allowing for better sensor geometry. This improved distribution of sensors results in lower HDOP values, indicating reduced potential for horizontal positioning errors. The IWR1642BOOST mmWave sensor, with its narrow 15° elevation field of view, poses a limitation on the distribution of sensors in the vertical plane. As a consequence, the accuracy of height estimation in 3-D positioning may be more susceptible to errors and uncertainties. Nevertheless, it was attempted to position four sensors at different heights (1, 1.5, 2, and 2.5 m) to demonstrate the potential improvement. Table II verifies this hypothesis by indicating significant improvement of algebraic solution in the z-axis (0.13 m) bringing the 3-D positioning error down to 0.31 m which is attributed to the significant improvement of the VDOP (average 1.54). Interestingly enough, it appears that the recursive solution fails to identify the optimal solution leading to significantly high errors. To further investigate the DOP significance we set up another experiment consisting of six anchors [the four anchors of the previous case plus one sensor at the ceiling (position **I**) and one on the floor (position **J**)]. This new constellation or anchors reduces both the VDOP as well as the HDOP and this reflected on both the multilateration approches. The average 3-D positioning error reduces down to 0.24 m while the one from the recursive version reduces down to 0.39 m. Interestingly, the standard algebraic solution still outperforms the recursive one, as can be seen in Table III.

b) 3-D triangulation approach: Considering the inaccuracy of the multilateration approach in the z-axis, particularly when DOP optimization is not possible, and capitalizing on the ability of the IWR1642BOOST sensor to measure the azimuth angle, the experimental setup was adjusted, deploying two sets of

TABLE I
FOUR-ANCHOR CONFIGURATION - EQUAL HEIGHT

Point	Distance Error(m)	Algebraic Multilateration				Recursive Multilateration				HDOP	VDOP
		XYZ Error(m)			3-D Error(m)	XYZ Error(m)			3-D Error(m)		
		x	y	z		x	y	z			
1	-0.04	0.12	0.23	0.08	0.27	0.02	-0.27	-1.02	1.05	1.12	43.05
2	-0.06	0.22	0.07	-9.46	9.46	0.28	-0.02	-1.23	1.26	1.10	25.95
3	0.09	0.12	0.00	-1.35	1.35	0.09	-0.12	0.36	0.39	1.11	4.95
4	0.03	-0.21	-0.09	0.43	0.49	-0.12	-0.22	4.77	4.78	1.11	8.35
5	-0.02	-0.22	0.12	-16.40	16.40	0.02	-0.26	2.39	2.40	1.06	4.95
6	0.10	-0.07	0.08	-11.11	11.11	0.00	-0.06	-1.68	1.68	1.11	10.59
7	-0.09	0.05	0.06	-6.56	6.56	0.39	0.09	1.54	1.59	1.24	44.70
8	-0.02	-0.13	-0.16	0.40	0.45	-0.22	0.17	-0.56	0.62	1.25	46.41
Average	***0.06***	***0.14***	***0.10***	***5.72***	***5.76***	***0.14***	***0.15***	***1.69***	***1.72***	**1.14**	**23.61**
Std Dev	***0.03***	***0.07***	***0.07***	***6.15***	***6.11***	***0.14***	***0.09***	***1.40***	***1.39***	**0.07**	**18.70**

The bold indicate Average and Standard Deviation Values.

TABLE II
FOUR-ANCHOR CONFIGURATION - DIFFERENT HEIGHT

Point	Distance Error(m)	Algebraic Multilateration				Recursive Multilateration				HDOP	VDOP
		XYZ Error(m)			3-D Error(m)	XYZ Error(m)			3-D Error(m)		
		x	y	z		x	y	z			
1	0.07	-0.19	-0.20	-0.15	0.32	-0.29	0.00	-0.37	0.47	1.07	1.80
2	0.05	-0.09	-0.25	0.03	0.27	0.28	-0.31	-0.12	0.44	1.06	1.61
3	-0.14	0.23	0.02	0.47	0.52	0.11	-0.09	-0.33	0.36	1.12	1.75
4	-0.06	-0.13	-0.29	0.12	0.34	-1.59	-0.02	1.94	2.51	1.31	1.49
5	-0.06	4.07	0.08	0.02	0.14	0.16	-2.94	-0.19	2.81	1.22	1.41
6	-0.12	0.21	0.07	0.03	0.22	-1.53	-0.27	1.96	2.50	1.07	1.03
7	0.13	0.06	-0.22	0.04	0.23	-0.39	-0.17	0.09	0.44	1.10	0.93
8	-0.07	-0.29	0.23	-0.11	0.38	0.13	0.27	-0.33	0.45	1.06	1.16
Average	***0.09***	***0.16***	***0.16***	***0.13***	***0.31***	***0.91***	***0.17***	***0.99***	***1.40***	**1.41**	**1.54**
Std Dev	***0.04***	***0.08***	***0.11***	***0.14***	***0.11***	***1.02***	***0.12***	***1.07***	***1.43***	**0.09**	**0.33**

The bold indicate Average and Standard Deviation Values.

TABLE III
SIX-ANCHOR CONFIGURATION - DIFFERENT HEIGHT

Point	Distance Error(m)	Algebraic Multilateration				Recursive Multilateration				HDOP	VDOP
		XYZ Error(m)			3-D Error(m)	XYZ Error(m)			3-D Error(m)		
		x	y	z		x	y	z			
1	0.00	-0.18	0.07	-0.56	0.59	-0.07	0.01	-0.14	0.15	0.93	1.60
2	-0.08	0.11	-0.05	-0.27	0.30	-0.12	-0.27	-0.06	0.30	0.95	1.63
3	0.04	-0.02	-0.03	0.17	0.17	0.64	0.01	0.67	0.93	0.93	1.70
4	-0.12	-0.04	0.11	-0.12	0.17	0.01	-0.34	-0.05	0.35	0.96	1.60
5	-0.02	-0.05	0.08	0.07	0.11	0.52	-0.15	0.03	0.55	0.93	1.44
6	-0.07	0.07	-0.03	0.07	0.10	-0.01	-0.14	-0.31	0.34	0.88	1.74
7	0.13	-0.08	-0.02	0.48	0.49	0.08	0.05	0.19	0.22	0.91	1.68
8	0.11	0.03	0.00	-0.01	0.03	0.24	0.10	0.10	0.28	0.95	1.45
Average	***0.07***	***0.07***	***0.05***	***0.22***	***0.24***	***0.21***	***0.13***	***0.19***	***0.39***	**0.94**	**1.48**
Std Dev	***0.05***	***0.05***	***0.04***	***0.20***	***0.20***	***0.24***	***0.12***	***0.21***	***0.25***	**0.03**	**0.11**

The bold indicate Average and Standard Deviation Values.

two sensors on top of each other, as shown in Fig. 3. Sensor **D** is placed on top of **A**, sensor **E** on top of **C**, while sensor **F** was left on its own on the far-most right corner. 3-D position estimation is achieved by using a combination of typical triangulation formulation using the azimuth angles measured from the three corners while the z-axis coordinate is estimated based on the height formulation (4) as follows, which estimates the height h in the complexity-reduced trilateration approach (COLA) approach presented in [37]. Although only four sensors are practically required to achieve 3-D positioning using this approach, our setup consists of five in three different corners. An absolute minimum requirement is that three azimuth measurements are collected from the three corners to estimate the x and y of the target while one pair of two sensors from one corner is needed to estimate the height. In our approach the pair which had a shorter horizontal distance to the estimated x, y of the target was selected to estimate the height using

$$h = z_2 - \frac{d_2^2 - d_1^2 + (z_2 - z_1)^2}{2(z_2 - z_1)}. \tag{4}$$

Results tabulated in Table IV indicate a significant improvement in the z-axis (0.11 m) while there is also a good improvement in the x and y axes (error being 0.09 and 0.08 m) bringing the 3-D positioning accuracy down to 0.17 m.

B. 3-DOF Sensor

Texas Instrument's IWR1843BOOST is considered as a newer upgrade to the IWR1642BOOST sensor used in the previous experiments. The additional antenna, enables the measurement

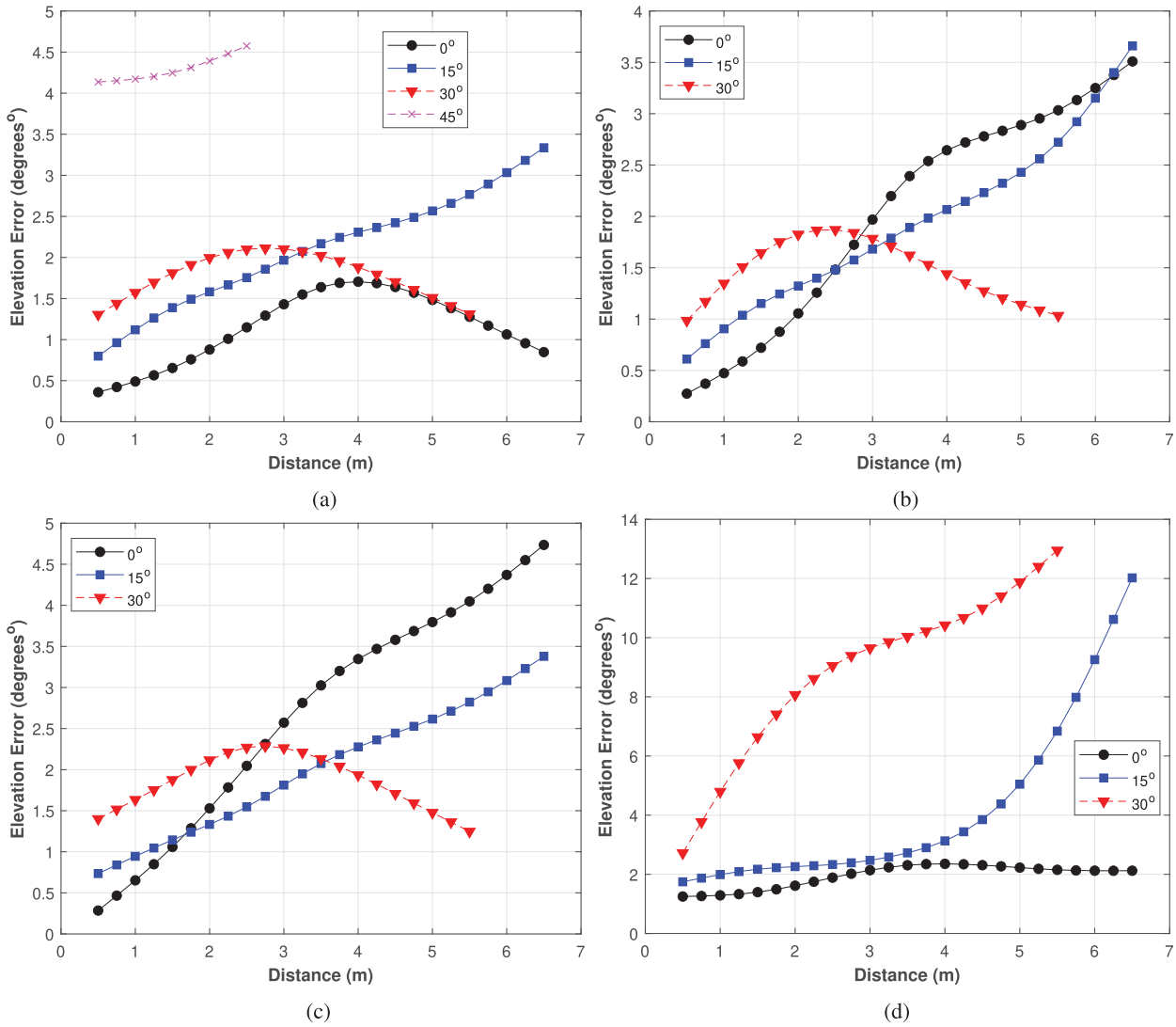

Fig. 10. IWR1843BOOST elevation accuracy. (a) 0° azimuth. (b) 15° azimuth. (c) 30° azimuth. (d) 45° azimuth.

TABLE IV
3-D TRIANGULATION POSITIONING

Point	Azimuth Error(°)	XYZ Error(m)			3-D Error(m)
		x	y	z	
1	1.02	0.13	0.14	-0.03	0.20
2	0.72	-0.03	0.09	0.16	0.19
3	0.91	-0.08	-0.09	0.14	0.19
4	1.88	-0.04	-0.13	0.16	0.22
5	1.51	0.25	0.11	-0.13	0.31
6	0.91	0.09	-0.08	-0.30	0.32
7	0.39	0.06	0.03	0.04	0.08
8	2.20	0.05	-0.02	-0.03	0.06
Average	***1.20***	***0.09***	***0.08***	***0.11***	***0.17***
St Dev	***0.61***	***0.04***	***0.04***	***0.09***	***0.09***

The bold indicate Average and Standard Deviation Values.

of the elevation angle in addition to the azimuth and range, facilitating 3-DOF. This, in theory, means that 3-D positioning could now be achieved using only one sensor. In this section, a precision analysis is conducted using the experimental setup described in Section IV-C2 as well as 3-D positioning experiment results using single- and multisensor configuration are showcased.

1) Precision Analysis: The aim of this analysis is to evaluate the elevation accuracy of the IWR1843BOOST sensor at different azimuths and distances. By inspecting Fig. 10, it can be observed that the elevation error across different azimuth angles follows a similar pattern, where the error gradually increases with an increase of the azimuth angle and the distance. At bore-sight [0°azimuth - Fig. 10(a)] the sensor measures the elevation quite accurately with the error ranging between 1–2° up to an elevation angle of 30°. Beyond an elevation angle of 30°, the sensor fails to provide elevation measurements at a distance beyond 2.5 m. Increasing the azimuth angle has a negative effect on the elevation measurement accuracy, as shown in Fig. 10(b)–10(d). It can then be concluded from these plots that the sensor demonstrates a fairly acceptable elevation measurement accuracy (averaging at 3°) within a vertical field of view of around 60° (−30° to +30°). That combined with the 90° azimuth field of view, illustrates that

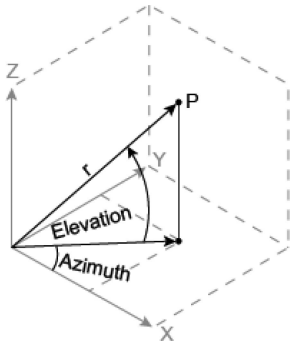

Fig. 11. Spherical to Cartesian conversion.

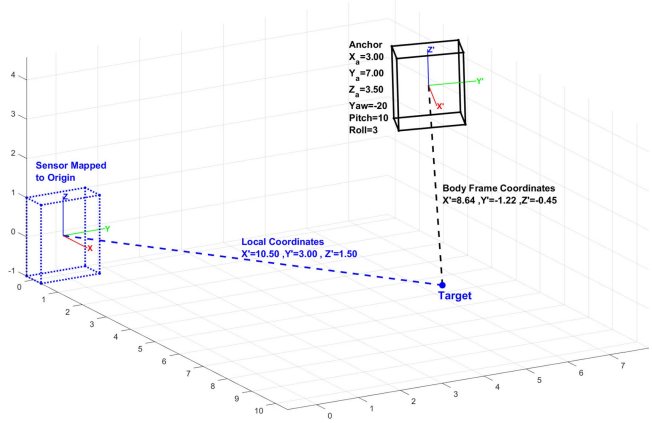

Fig. 12. Body frame to local coordinates conversion.

the sensor could cover the majority of the room if placed in the corner.

2) 3-DOF Sensor 3-D Positioning: Following the IWR18-43BOOST elevation precision analysis, it is worth capitalizing on the ability of the sensor to measure elevation in addition to azimuth and range to perform 3-D positioning using a single anchor.

a) 3-DOF single-anchor 3-D positioning: To analyze the positioning accuracy when a single IWR1843BOOST sensor is used, a similar approach to that used in the precision analysis was adopted. This involved a drone flying in front of the sensor while the sensor was incrementally rotated to vary both azimuth and elevation angles. This experiment was conducted at various distances from the sensor to capture data across a range of positions. Having available, the range(r), the azimuth(θ), and the elevation(ϕ) measurements from the anchor to the target, one can estimate the coordinates of the target with respect to the body-frame coordinate system of the anchor using a standard spherical to the Cartesian coordinate conversion according to Fig. 11 and the following equation:

$$\begin{bmatrix} x' \\ y' \\ z' \end{bmatrix} = r \begin{bmatrix} \cos(\theta)\cos(\phi) \\ \cos(\theta)\sin(\phi) \\ \sin(\theta) \end{bmatrix}. \tag{5}$$

To properly determine the coordinates of the target within the room's coordinate plane, it was imperative to align the coordinate system of the sensor (body frame coordinate system) to that of the room (local coordinate system). Achieving this alignment involves a series of calculations that account for the sensor's yaw, pitch, and roll. These adjustments were critical in ensuring that the sensor's data correspond accurately to the room's coordinate plane, allowing for reliable 3-D positioning. Assuming that the anchor is first rotated by an angle ψ around the z-axis (yaw), then by an angle θ around y-axis (pitch), and finally by an angle ϕ around the x-axis (roll) the 3×3 rotation matrix is given by

$$\mathrm{R} = R_z \cdot R_y \cdot R_x \tag{6}$$

where

$$R_x = \begin{bmatrix} 1 & 0 & 0 \\ 0 & \cos(\phi) & -\sin(\phi) \\ 0 & \sin(\phi) & \cos(\phi) \end{bmatrix}$$

$$R_y = \begin{bmatrix} \cos(\theta) & 0 & \sin(\theta) \\ 0 & 1 & 0 \\ -\sin(\theta) & 0 & \cos(\theta) \end{bmatrix}$$

$$R_z = \begin{bmatrix} \cos(\psi) & -\sin(\psi) & 0 \\ \sin(\psi) & \cos(\psi) & 0 \\ 0 & 0 & 1 \end{bmatrix}. \tag{7}$$

With reference to Fig. 12 and considering that body-frame measurement from a sensor positioned at $A = [x_a y_a z_a]$ is $P' = [x'y'z']$ then the local coordinates $P = [xyz]$ of the target can be calculated using

$$\mathrm{P} = [R \cdot P'^T]^T + A. \tag{8}$$

The IWR1843BOOST was used to conduct a single sensor 3-D positioning experiment, evaluating its performance over a distance of 6.5 m. The evaluation revealed a varying level of accuracy contingent on azimuth and elevation angles. With reference to the results presented in Fig. 13, when the sensor was aligned at 0°azimuth, it demonstrated exceptional 3-D accuracy which was slowly increasing as the distance and elevation from the target were increased. As it was expected, at large elevation angles (e.g., 45°) and at long distances the sensor was failing to provide a measurement. This is indicated by the gaps in the surface plots in Fig. 13. The contour plots at the bottom of each surface plot indicate the range of distance/elevation values that the error is below an intuitively selected accepted 3-D positioning error (0.4 m). As it was expected the positioning accuracy appears to deteriorate faster as the azimuth angle starts increasing limiting the usability and reliability of the sensors at very low elevation and azimuth maximums. In a scenario where multiple sensors are used, one could use the range, azimuth, and elevation measurements as a measure of the reliability of the single-anchor position estimation and either use or discard the particular anchor from the entire positioning algorithm.

This adaptability in adjusting the sensor's coordinate system, regardless of its orientation, proved to be a pivotal advantage. It enabled us to place and orient the sensor in positions that were previously challenging due to issues related to sensor clustering. This flexibility allowed us to direct the sensor toward

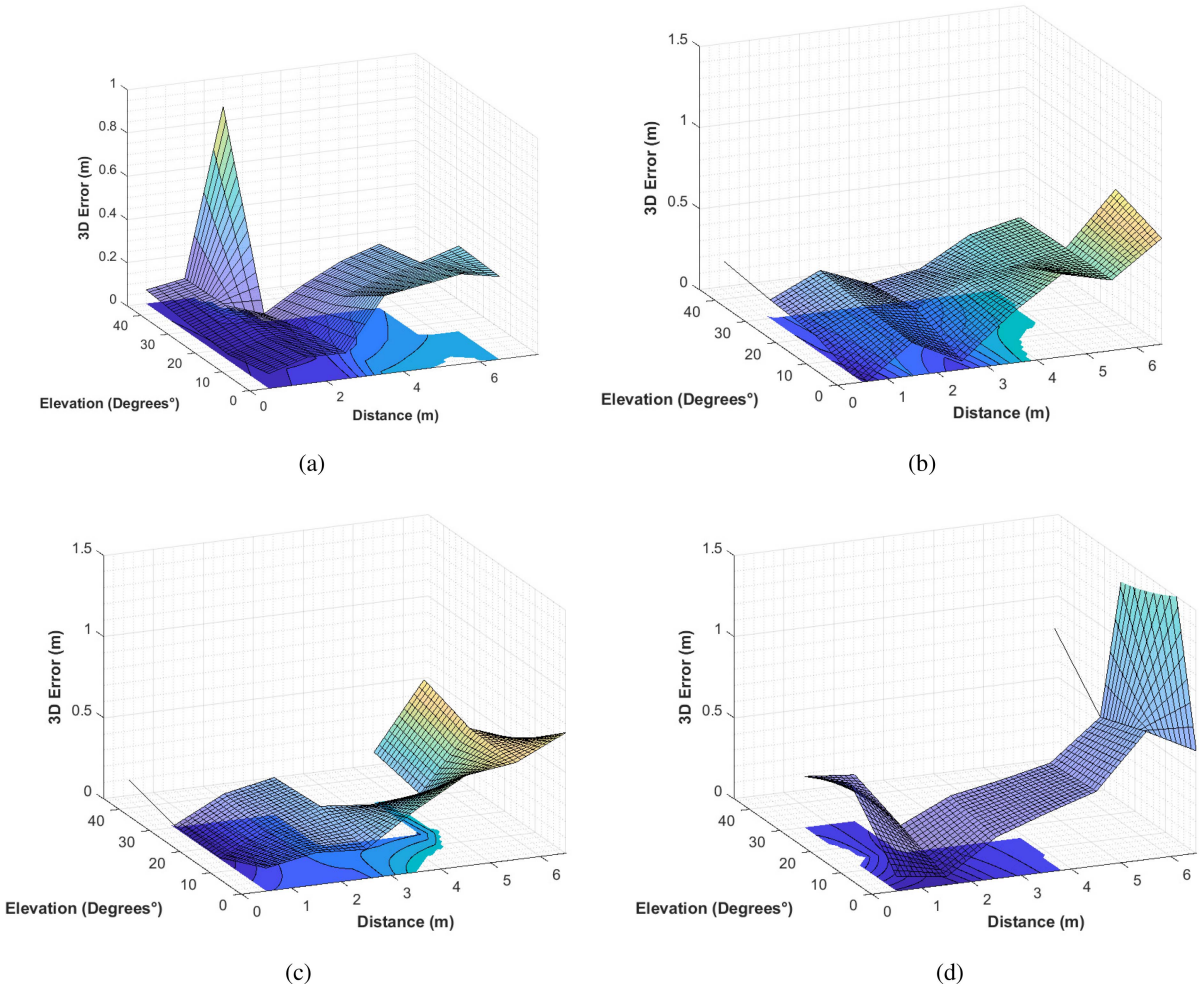

Fig. 13. IWR1843BOOST single sensor positioning accuracy. (a) 0° azimuth. (b) 15° azimuth. (c) 30° azimuth. (d) 45° azimuth.

unconventional angles, such as placing it on the ceiling facing downward or on the floor facing upward.

b) 3-DOF multianchor 3-D positioning: In this experiment, a 3-DOF multianchor 3-D positioning system was implemented using IWR1832BOOST mmWave sensors. The study involved the use of five sensors, in the environment shown in Fig. 5, where two distinct setups were tested, each with slight variations. In Setup A, one sensor was placed lower than the others and faced upward, while in Setup B, a sensor was positioned higher than the rest and faced downward. Both configurations were rigorously examined using three different approaches: 1) an averaged multianchor positioning approach, 2) a classical multilateration approach, and 3) a multiangulation approach using angle of departure (AoD). The obtained results can be seen in Table V. The experiment consisted of a drone hovering over multiple randomly selected points at various heights. Each of the sensors would capture and position the drone, outputting the 3-D coordinates (xyz) using the single-anchor positioning approach presented in the previous paragraph (V-B2a) as well as the azimuth and elevation angling and ranging data for the triangulation and multilateration approaches, respectively. As shown in Section V-B2a, it is possible to achieve the 3-D position using only one 3-DOF mmWave sensor, however, this setup consisted of five, the position estimates of which were averaged to estimate the final drone position.

Averaged Multianchor Approach: Capitalizing on the capability of the IWR1843BOOST sensor to perform single-angle positioning the averaged approach consists of utilizing more than one (five in this experiment) while having their estimates averaged to estimate the target position. Our algorithm involved discarding estimates which appeared as outliers or they have been estimated using measurements at long distances, high azimuth, and elevation angles which we observed in the precision analysis are likely to cause large positioning errors. The outcomes demonstrated a remarkable precision, with an error of approximately 17 cm observed using Setup A and 16 cm using Setup B. The minimal disparity between the results of the two setups indicates the robustness of the system. However, it can be observed from Table V that the configuration where one sensor was positioned on top facing downward exhibited superior results in the z-axis compared to the alternative setup. Qualitatively, we can also report that we observed that Setup B resulted in less sensor failures, resulting in more estimates being considered in the averaging process and the final calculation of the target position. Fig. 14 is a visual demonstration of the positioning accuracy achieved using Setup B when the drone

TABLE V
3-DOF MULTIANCHOR 3D POSITIONING RESULTS

Point	Averaged Approach				Multilateration Approach				Multiangulation Approach				Sensor Setup
	XYZ Error(m)			3-D Error(m)	XYZ Error(m)			3-D Error(m)	XYZ Error(m)			3-D Error(m)	
	x	y	z		x	y	z		x	y	z		
Setup A													
1	0.11	0.02	0.22	0.25	0.10	0.04	0.25	0.27	0.01	0.21	0.25	0.33	A
2	0.09	0.20	0.01	0.22	0.30	0.16	0.46	0.57	0.32	0.04	0.06	0.33	Y:45^o,P:15^o,R:0^o
3	0.01	0.02	0.10	0.10	0.15	0.04	0.05	0.16	0.04	0.05	0.16	0.18	B
4	0.06	0.09	0.07	0.13	0.32	0.02	0.62	0.70	0.17	0.07	0.15	0.23	Y:0^o,P:-30^o,R:0^o
5	0.09	0.14	0.01	0.17	0.09	0.10	0.31	0.34	0.10	0.00	0.06	0.11	C
6	0.00	0.12	0.14	0.18	0.16	0.09	0.08	0.20	0.18	0.02	0.21	0.27	Y:-45^o,P:15^o,R:0^o
7	0.08	0.06	0.01	0.10	0.05	0.06	0.09	0.12	0.07	0.08	0.06	0.12	D
8	0.04	0.09	0.12	0.16	0.10	0.09	0.01	0.13	0.24	0.07	0.21	0.33	Y:-90^o,P:15^o,R:0^o
9	0.07	0.11	0.02	0.13	0.03	0.09	0.08	0.13	0.02	0.05	0.09	0.11	E
Average	***0.07***	***0.10***	***0.09***	***0.17***	***0.14***	***0.08***	***0.21***	***0.21***	***0.13***	***0.07***	***0.14***	***0.22***	Y:90^o,P:15^o,R:0^o
St Dev	***0.04***	***0.05***	***0.08***	***0.05***	***0.10***	***0.04***	***0.21***	***0.21***	***0.11***	***0.06***	***0.07***	***0.10***	
Setup B													
1	0.02	0.11	0.02	0.11	0.24	0.04	0.56	0.61	0.14	0.02	0.03	0.14	B
2	0.03	0.09	0.09	0.13	0.26	0.00	0.15	0.30	0.23	0.13	0.17	0.31	Y:31^o,P:15^o,R:0^o
3	0.02	0.00	0.13	0.13	0.16	0.04	0.73	0.75	0.04	0.19	0.21	0.29	C
4	0.08	0.02	0.08	0.11	0.42	0.15	0.66	0.79	0.20	0.20	0.17	0.33	Y:-58^o,P:15^o,R:0^o
5	0.13	0.02	0.02	0.13	0.09	0.11	0.30	0.34	0.06	0.11	0.06	0.14	D
6	0.24	0.02	0.01	0.24	0.43	0.05	0.56	0.71	0.37	0.00	0.08	0.38	Y:-121^o,P:15^o,R:0^o
7	0.28	0.14	0.05	0.32	0.19	0.14	1.28	1.30	0.13	0.14	0.13	0.23	E
8	0.01	0.18	0.02	0.18	0.11	0.19	1.17	1.19	0.04	0.19	0.05	0.20	Y:117^o,P:15^o,R:0^o
9	0.06	0.02	0.08	0.10	0.11	0.01	1.75	1.75	0.24	0.12	0.01	0.27	F
Average	***0.10***	***0.06***	***0.05***	***0.16***	***0.22***	***0.08***	***0.79***	***0.86***	***0.16***	***0.12***	***0.10***	***0.25***	Y:-180^o,P:30^o,R:0^o
St Dev	***0.10***	***0.06***	***0.04***	***0.07***	***0.13***	***0.06***	***0.51***	***0.47***	***0.11***	***0.07***	***0.07***	***0.08***	

Y: yaw, P: pitch, R: roll.
The bold indicate Average and Standard Deviation Values.

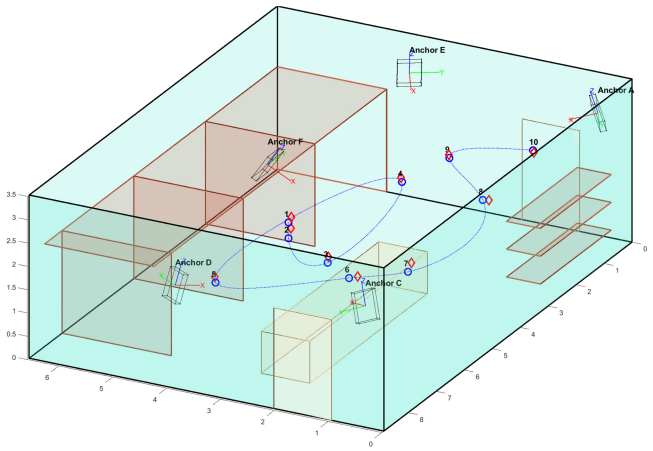

Fig. 14. 3-D positioning using multiple 3-DOF mmWave anchors. Blue circles indicate ground truths and red diamonds estimated positions.

was flown along the trajectory indicated with a blue dotted line. Ground truth locations were available at the points indicated with a blue circle while red diamonds are the actual position estimates. Comparing these findings to a 2-DOF 3-D triangulation approach presented in Section V-A2b , it is noteworthy that the results were very similar, with a 3-D error of approximately 17 cm also. Overall, this experiment showcases the potential and reliability of the implemented system in real-world applications requiring precise 3-D object localization.

Multilateration Approach: Using the ranging information from at least four sensors, we were able to establish the 3-D position of the target using multilateration similarly to the approach described in Section V-A2. The results demonstrated a 3-D error of 0.21 m using Setup A and 0.86 m using Setup B. It can be seen that the higher errors compared to the averaged approach are mostly due to high errors in the z-axis, especially using Setup B. These errors are due to the fact that the sensors are positioned at relatively similar heights compared to Setup A, where one sensor is positioned much lower and aimed looking up. This leads to a worsened distribution of the sensors vertically and therefore higher VDOP which, as discussed in Section III-A5, leads to poor multilateration performance.

Multiangulation Approach: To implement the AoD approach, angling information (azimuth and elevation) from at least three sensors to the target is required to establish the 3-D position of the targeted object. The formulation of this approach can be found in [38]. As it can be seen in Table V, the average 3-D error using the AoD approach was calculated to be around 0.22 m using Setup A and around 0.25 m using Setup B.

C. Discussion

1) 2-DOF Case: The results of the 2-DOF precision analysis and positioning estimations highlight the potential of mmWave technology for achieving range and angle measurement precision and thereafter high 3-D positioning accuracy. The precision analysis revealed that out of the two sensor types that were used the Texas Instruments sensor outperformed the Infineon one in terms of range and angle measurement precision at a wider field of view. Due to the fact that the Infineon sensor is only able to identify objects up to a 20° angle, it becomes evident that this sensor is not appropriate for a system where at least four sensors are required to cover the visibility of an entire room. On the other hand, TI sensor has shown very promising results, showcasing

ranging precision of 0.17 m at 0° and a capability of identifying an object at 60° with an accuracy of 0.3 m up to 6 m.

The 3-D positioning estimation using the 2-DOF sensor was done using both a 3-D multilateration and a triangulation approach. The multilateration approach demonstrated a relatively high 3-D positioning error of 0.8 m in the z-axis estimation. This indicated the challenges associated with accurately estimating the z-axis using multilateration alone. To address these limitations in z-axis estimation, a 2-D triangulation approach utilizing azimuth angles from three sensors was used combined with a lateration approach to estimate the height utilizing sensors placed on top of each other. Although only one additional sensor is required to be placed at a higher altitude above one of the existing sensors to be able to estimate the height, we have deployed two sets at the two corners of the room to ensure sufficient measurements in case one of these fails to return measurements due to either blockages or long distances. This modification in the sensor setup resulted in a reduction of the z-axis error down to 0.11 m, leading to an overall decrease in the 3-D positioning error down to 0.17 m. The errors in the x and y axes also improved, indicating the effectiveness of the triangulation approach in precise 3-D positioning estimation.

2) 3-DOF Case: Transitioning to the 3-DOF sensor, the limitations encountered with the 2-DOF sensor, including the implementation requirements of various multilateration and triangulation techniques, were overcome by leveraging the enhanced capabilities of the 3-DOF sensor to measure the elevation of the target in addition to the distance and azimuth. This sensor streamlined the 3-D positioning process by directly outputting the 3-D coordinates of the detected object, eliminating the need for intricate multistep methodologies. While the precision analysis demonstrated comparable results to the 2-DOF sensor, a significant advancement was noted in the expanded field of view. The 3-DOF sensor introduced an elevation angle measurement capability, enabling single-anchor 3-D positioning, offering more comprehensive spatial coverage when multiple sensors are placed around the room. The utilization of multiple 3-DOF anchors demonstrated a 3-D positioning accuracy of 16 cm as well as notably improved the system's efficiency, leading to quicker response times and smoother overall functionality. Comparing this approach to classical multilateration and triangulation approaches has indicated that not only this approach had better results but also offers much flexibility as its algebraic implementation does not impose limitations in terms of the number of required sensors (four for the multilateration and three for the triangulation). This is practically a significant benefit as in a practical scenario the cost of implementing a 3-D positioning system could be significantly reduced.

Comparing the results mentioned in Section II with the findings in [17] and [15], it is evident that our approaches yielded a similar level of accuracy. In [17], the authors achieved positioning accuracy ranging from 16 cm to 3.25 m using the AoA technique in an open space, while the authors of [15] demonstrated an accuracy of 15 cm. Despite the fact that we were operating in a more cluttered environment, we achieved an accuracy of 16 cm, which is comparable to the aforementioned works.

VI. Conclusion

In this article, we have demonstrated the potential of mmWave radar sensory technology to be used for accurate cm-level 3-D indoor localization. To explore its full capabilities, we have compared mmWave sensor from two vendors (Texas Instruments, Infineon) while we specifically compared the positioning potential of two types of sensors with different degrees of freedom: one that measures distance and azimuth angle to the target (2-DOF) and another one that additionally measures elevation (3-DOF). The measurement precision analysis and experimental positioning results indicate promising capabilities of both systems in achieving accurate 3-D positioning. Using a 2-DOF sensor system we have achieved a 3-D positioning accuracy of 17 cm using a 3-D trilateration approach, whereas with a 3-DOF sensor system we achieved a very similar accuracy averaging at 16 cm in a multianchor setup with some enhanced robustness and flexibility in implementation.

Despite this high accuracy, the technology imposes several challenges, difficulties, and limitations when it comes to setting up and using a multisensor positioning system. These challenges include sensing limitations of mmWave sensors, the difficulty of detecting stationary targets, the complexity of multiobject detection, and the need for timing synchronization. These challenges were addressed through careful system design and the implementation of appropriate solutions.

References

[1] C. Han, X. Zhu, A. Doufexi, and T. Kocak, "Location-aided multi-user beamforming for 60 GHz WPAN systems," in *Proc. IEEE 75th Veh. Technol. Conf.*, 2012, pp. 1–5.

[2] J. Yang, H. Lee, and K. Moessner, "Multilateration localization based on singular value decomposition for 3D indoor positioning," in *Proc. Int. Conf. Indoor Positioning Indoor Navigation*, 2016, pp. 1–8.

[3] Y. Li, W. Nie, W. He, Y. Wang, and X. Yang, "UAV 3D localization system using CSI," in *Proc. Int. Conf. Microw. Millimeter Wave Technol.*, 2021, pp. 1–3.

[4] Y. Yu et al., "Precise 3-D indoor localization based on Wi-Fi FTM and built-in sensors," *IEEE Internet Things J.*, vol. 7, no. 12, pp. 11753–11765, Dec. 2020.

[5] H. Cao, Y. Wang, and J. Bi, "Smartphones: 3D indoor localization using Wi-Fi RTT," *IEEE Commun. Lett.*, vol. 25, no. 4, pp. 1201–1205, Apr. 2021.

[6] L. Pei, R. Chen, J. Liu, T. Tenhunen, H. Kuusniemi, and Y. Chen, "An inquiry-based bluetooth indoor positioning approach for the Finnish pavilion at Shanghai World Expo 2010," in Proc. IEEE/ION Position Location Navigation Symp., 2010, pp. 1002–1009.

[7] Q. Liang, J. Lin, and M. Liu, "Towards robust visible light positioning under led shortage by visual-inertial fusion," in *Proc. Int. Conf. Indoor Positioning Indoor Navigation*, 2019, pp. 1–8.

[8] K. Mannay, J. Ureña, A. Hernández, M. Machhout, and T. Aguili, "Characterization of an ultrasonic local positioning system for 3D measurements," *Sensors*, vol. 20, no. 10, 2020, Art. no. 2794.

[9] A. Mandal, C. Lopes, T. Givargis, A. Haghighat, R. Jurdak, and P. Baldi, "Beep: 3D indoor positioning using audible sound," in *Proc. IEEE 2nd Consum. Commun. Netw. Conf.*,2005, pp. 348–353.

[10] A. Sesyuk, S. Ioannou, and M. Raspopoulos, "A survey of 3D indoor localization systems and technologies," *Sensors*, vol. 22, no. 23, 2022, Art. no. 9380.

[11] D. Wang, M. Fattouche, and X. Zhan, "Pursuance of mm-level accuracy: Ranging and positioning in mmWave systems," *IEEE Syst. J.*, vol. 13, no. 2, pp. 1169–1180, Jun. 2019.

[12] A. Sesyuk, S. Ioannou, and M. Raspopoulos, "3D millimeter-wave indoor localization," in *Proc. 13th Int. Conf. Indoor Positioning Indoor Navigation*, 2023, pp. 1–7.

[13] Y. Jia, H. Tian, S. Fan, and B. Liu, "Motion feature and millimeter wave multi-path AoA-ToA based 3D indoor positioning," in *Proc. IEEE 29th Annu. Int. Symp. Pers. Indoor Mobile Radio Commun.*, 2018, pp. 1–7.
[14] Y. Wang, K. Zhao, and Z. Zheng, "A 3D indoor positioning method of wireless network with single base station in multipath environment," *Wireless Commun. Mobile Comput.*, vol. 2022, 2022, Art. no. 3144509.
[15] Z. Hao, H. Yan, X. Dang, Z. Ma, P. Jin, and W. Ke, "Millimeter-wave radar localization using indoor multipath effect," *Sensors*, vol. 22, 2022, Art. no. 5671.
[16] A. Antonucci et al., "Performance analysis of a 60-GHz radar for indoor positioning and tracking," in *Proc. Int. Conf. Indoor Positioning Indoor Navigation*, 2019, pp. 1–7.
[17] O. Kanhere and T. S. Rappaport, "Position locationing for millimeter wave systems," in *Proc. IEEE Glob. Commun. Conf.*, 2018, pp. 206–212, doi: 10.1109/GLOCOM.2018.8647983.
[18] Z. Lin, T. Lv, and P. T. Mathiopoulos, "3-D indoor positioning for millimeter-wave massive MIMO systems," *IEEE Trans. Commun.*, vol. 66, no. 6, pp. 2472–2486, Jun. 2018.
[19] T. Wu et al., "RIS-aided localization algorithm and analysis: Tackling non-Gaussian angle estimation errors," 2022. [Online]. Available: https://api.semanticscholar.org/CorpusID:253420801
[20] Y. Cui, H. Yin, L. Tan, and M. D. Renzo, "A 3D positioning-based channel estimation method for RIS-aided mmWave communications," 2022, *arXiv:2203.14636*.
[21] M. Lam, L. Dodds, A. Eid, J. Hester, and F. Adib, "3D self-localization of drones using a single millimeter-wave anchor," 2023, *arXiv:2310.08778*.
[22] S. Dogru and L. Marques, "Pursuing drones with drones using millimeter wave radar," *IEEE Robot. Automat. Lett.*, vol. 5, no. 3, pp. 4156–4163, Jul. 2020.
[23] O. Kolawole and M. Hunukumbure, "A drone-based 3D localization solution for emergency services," in *Proc. IEEE Int. Conf. Commun.*, 2022, pp. 1–6.
[24] F. Parralejo, J. A. Paredes, F. J. Aranda, F. J. Álvarez, and J. A. Moreno, "Millimetre wave radar system for safe flight of drones in human-transited environments," in *Proc. 13th Int. Conf. Indoor Positioning Indoor Navigation*, 2023, pp. 1–6.
[25] P. K. Rai et al., "Localization and activity classification of unmanned aerial vehicle using mmWave FMCW radars," *IEEE Sensors J.*, vol. 21, no. 14, pp. 16043–16053, Jul. 2021.
[26] A. Shahmansoori, G. E. Garcia, G. Destino, G. Seco-Granados, and H. Wymeersch, "Position and orientation estimation through millimeter-wave MIMO in 5G systems," *IEEE Trans. Wireless Commun.*, vol. 17, no. 3, pp. 1822–1835, Mar. 2018.
[27] Y. Han, Y. Shen, X.-P. Zhang, M. Z. Win, and H. Meng, "Performance limits and geometric properties of array localization," *IEEE Trans. Inf. Theory*, vol. 62, no. 2, pp. 1054–1075, Feb. 2016.
[28] G. Ciattaglia, G. Iadarola, L. Senigagliesi, S. Spinsante, and E. Gambi, "UAV propeller rotational speed measurement through FMCW radars," *Remote Sens.*, vol. 15, no. 1, 2023, Art. no. 270.
[29] B. Antonescu, M. Tehrani Moayyed, and S. Basagni, "Clustering algorithms and validation indices for a wide mmWave spectrum," *Information*, vol. 10, no. 9, 2019, Art. no. 287.
[30] H. He, Y. Liang, and S. Li, "Clustering algorithm based on azimuth in mmWave massive MIMO-NOMA system," in *Proc. IEEE/CIC Int. Conf. Commun. China (ICCC Workshops)*, 2021, pp. 118–122.
[31] M. T. Moayyed, B. Antonescu, and S. Basagni, "Clustering algorithms and validation indices for mmWave radio multipath propagation," in *Proc. Wireless Telecommun. Symp.*, 2019, pp. 1–7.
[32] V. Kathiresan and P. Sumathi, "An efficient clustering algorithm based on Z-score ranking method," in *Proc. Int. Conf. Comput. Commun. Inform.*, 2012, pp. 1–4.
[33] M. Wang, Z. Chen, Z. Zhou, J. Fu, and H. Qiu, "Analysis of the applicability of dilution of precision in the base station configuration optimization of ultrawideband indoor TDOA positioning system," *IEEE Access*, vol. 8, pp. 225076–225087, 2020.
[34] B. Li, K. Zhao, and X. Shen, "Dilution of precision in positioning systems using both angle of arrival and time of arrival measurements," *IEEE Access*, vol. 8, pp. 192506–192516, 2020.
[35] F. Malivert, O. Labbani-Igbida, and H. Boeglen, "Comparison and improvement of 3D-multilateration for solving simultaneous localization of drones and UWB anchors," *Appl. Sci.*, vol. 13, no. 2, 2023, Art. no. 1002.
[36] A. Norrdine, "An algebraic solution to the multilateration problem," in *Proc. Int. Conf. Indoor Positioning Indoor Navigation*, 2012, pp. 1–5.
[37] C.-Y. Shih and P. J. Marrón, "COLA: Complexity-reduced trilateration approach for 3D localization in wireless sensor networks," in *Proc. 4th Int. Conf. Sensor Technol. Appl.*, 2010, pp. 24–32.
[38] X. Wei, N. Palleit, and T. Weber, "AOD/AOA/TOA-based 3D positioning in NLOS multipath environments," in *Proc. IEEE 22nd Int. Symp. Pers. Indoor Mobile Radio Commun.*, 2011, pp. 1289–1293.

Andrey Sesyuk (Student Member, IEEE) received the B.Eng. degree in electrical and electronic engineering, in 2020, from the University of Central Lancashire, Larnaca, Cyprus, where he is currently working toward the Ph.D. degree in indoor localization and navigation.

Since 2020, he has been working on 3-D indoor localization with the University of Central Lancashire, where he is also currently a Junior Researcher with INSPIRE Research Centre. His research interests include telecommunications and mobile wireless communications and technologies, electronic positioning/localization/tracking of wireless devices, image processing and computer vision, and IoT.

Stelios Ioannou (Member, IEEE) received the M.Sc. degree in electrical engineering, and a minor in engineering management, from University of South Florida (USF), Tampa, FL, USA, in 2004, and the Ph.D. degree in the optimization and control of energy and power systems for unmanned robotic systems from Unmanned Systems Lab, USF, in 2008.

Between 2005 and 2008, he has been a Ph.D. Researcher with the Clean Energy Research Centre and the Unmanned Systems Lab, USF. He was a Postdoctoral Fellow with the Cyprus Institute (2009–2012) and an Associate Research Scientist with the Unmanned Systems Research Laboratory (2012–2015) on Autonomous Flying Platforms for Atmospheric and Earth Surface Observations. From 2015 to 2018, he worked in the industry as an Electrical Engineer, on the design and supervision of commercial and residential electrical installations. In 2018, he was appointed as a Lecturer of electrical and electronic engineering with University of Central Lancashire, Cyprus campus, Pyla, and a Researcher with the INSPIRE Research Centre. He holds a patent, and authored or coauthored several publications in national and international conferences and journals. His research interests include multidisciplinary research involving unmanned ground vehicles (UGV) and unmanned aerial systems (UAS), optimization of energy and power systems, power quality, electronics, and embedded systems.

Marios Raspopoulos (Member, IEEE) received the M.Eng. degree in electronics and mobile technologies, the M.Sc. degree in communication networks and software, and the Ph.D. degree in telecommunication from the University of Surrey, Surrey, U.K, in 2003, 2004, and 2008, respectively.

Between 2004–2008, he was a Ph.D. Researcher with the Centre for Communications and Systems Research, University of Surrey. From 2008 to 2015, he was working for the industry, being the CTO at a Telecommunication firm, and managing the research and development activities. In 2015, he was appointed as an Assistant Professor with University of Central Lancashire (UCLan), Larnaca, Cyprus. He has been an Associate Professor, being the coordinator for the Electrical, Electronic, and Computer Engineering programmes, and deputy Head of the School of Sciences, and a Senior Researcher with INSPIRE Research Centre, UCLan Cyprus, since 2021. He has been heavily involved with engineering and telecommunication projects in areas like radio propagation/radio planning, electromagnetism, RF/antenna design, and wireless channel modeling, but has also expanded in other areas of information and communications technology (ICT) research, like localization and tracking, information technologies, etc. His research interests include the wide spectrum of ICT with special focus in telecommunications and mobile wireless communications and technologies.